

AD-A082 463

CALIFORNIA INST OF TECH PASADENA DIV OF CHEMISTRY A--ETC F/G 7/4
THE ADSORPTION OF FORMIC ACID ON Y ZEOLITES: AN INFRARED ABSORB--ETC(U)
MAR 80 T M DUNCAN, R W VAUGHAN N00014-75-C-0960

UNCLASSIFIED

TR-16

NL

1 OF 1

AD
2000 01 3



END

DATE

FILED

5-80

DTIC



LEVEL II

ADA 082463

OFFICE OF NAVAL RESEARCH
Contract N00014-75-C-0960

Technical Report #16

The Adsorption of Formic Acid on Y Zeolites: An Infrared Absorbance Study

T. M. Duncan and R. W. Vaughan
Division of Chemistry and Chemical Engineering
California Institute of Technology
Pasadena, California 91125

March, 1980

DTIC
ELECTE
S APR 2 1980 D
B

Reproduction in whole or in part is permitted for
any purpose of the United States Government

Approval for Public Release; Distribution Unlimited

Submitted to the Journal of Catalysis

DOC FILE COPYJ

80 3 26 004

UNCLASSIFIED

SECURITY CLASSIFICATION OF THIS PAGE (When Data Entered)

| REPORT DOCUMENTATION PAGE | | READ INSTRUCTIONS BEFORE COMPLETING FORM |
|--|-----------------------|--|
| 1. REPORT NUMBER ⑨ Technical Report 16 | 2. GOVT ACCESSION NO. | 3. RECIPIENT'S CATALOG NUMBER |
| 4. TITLE (and Subtitle) ⑥ The Adsorption of Formic Acid on Y Zeolites: An Infrared Absorbance Study | | 5. TYPE OF REPORT & PERIOD COVERED |
| 7. AUTHOR(s) ⑩ T. M. Duncan ● R. W. Vaughan | | 6. PERFORMING ORG. REPORT NUMBER |
| 9. PERFORMING ORGANIZATION NAME AND ADDRESS California Institute of Technology Division of Chemistry and Chemical Engineering Pasadena, California 91125 | | 8. CONTRACT OR GRANT NUMBER(s) ⑬ N00014-75-C-0960 |
| 11. CONTROLLING OFFICE NAME AND ADDRESS Office of Naval Research Chemistry Program Office Arlington, VA 22217 | | 10. PROGRAM ELEMENT, PROJECT, TASK AREA & WORK UNIT NUMBERS ⑫ 37 |
| 14. MONITORING AGENCY NAME & ADDRESS (if different from Controlling Office) ⑭ TR-26 | | 13. REPORT DATE ⑪ Mar 80 |
| | | 14. NUMBER OF PAGES 27 |
| | | 15. SECURITY CLASS. (of this report) Unclassified |
| | | 15a. DECLASSIFICATION/DOWNGRADING SCHEDULE |
| 16. DISTRIBUTION STATEMENT (of this Report) Approved for Public Release; Distribution Unlimited | | |
| 17. DISTRIBUTION STATEMENT (of the abstract entered in Block 20, if different from Report) | | |
| 18. SUPPLEMENTARY NOTES Preprint; submitted to the Journal of Catalysis | | |
| 19. KEY WORDS (Continue on reverse side if necessary and identify by block number) Catalysis, infrared absorbance, formic acid, zeolites, molecular sieves, dehydration reaction | | |
| 20. ABSTRACT (Continue on reverse side if necessary and identify by block number) The adsorption of formic acid on an ammonium-Y (NH ₄ -Y) zeolite and an ultrastable hydrogen-Y (H-Y) zeolite has been studied with transmission infrared spectroscopy. The formic acid is determined to be chemically adsorbed on both zeolites as bidentate formate ions and as covalently bonded unidentate formate species. Assuming uniform infrared extinction coefficients for the two adsorbed formates, the NH ₄ -Y zeolite has comparable amounts of each surface species. The ultrastable H-Y zeolite, which has enhanced | | |

DD FORM 1 JAN 73 1473

EDITION OF 1 NOV 65 IS OBSOLETE
S/N 0102-LP-014-6601

UNCLASSIFIED 072575
SECURITY CLASSIFICATION OF THIS PAGE (When Data Entered)

UNCLASSIFIED

SECURITY CLASSIFICATION OF THIS PAGE (When Data Entered)

catalytic properties, adsorbs the formic acid primarily as bidentate formate ions. It is suggested that the nonframework aluminum cations in the ultra-stable H-Y zeolite act as adsorption sites for the formate ions.

| | |
|---------------------------------|---|
| ACCESSION for | |
| NTIS | White Section <input checked="" type="checkbox"/> |
| DOC | Buff Section <input type="checkbox"/> |
| UNANNOUNCED | <input type="checkbox"/> |
| JUSTIFICATION _____ | |
| BY _____ | |
| DISTRIBUTION/AVAILABILITY CODES | |
| Dist. | AVAIL. and/or SPECIAL |
| A | |

UNCLASSIFIED

SECURITY CLASSIFICATION OF THIS PAGE (When Data Entered)

I. INTRODUCTION

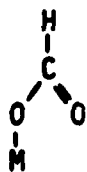
Formic acid decomposes catalytically by dehydration to H_2O and CO or by dehydrogenation to H_2 and CO_2 depending on the nature of the catalyst (1,2). Metals, such as Cu or Ni , catalyze primarily the dehydrogenation reaction. On metal oxides both reactions may occur to some degree. However, on aluminas and silicas the dehydration reaction dominates (2).

We present here a study of the adsorption of formic acid on two zeolites: an ammonium-Y ($\text{NH}_4\text{-Y}$) and an ultrastable hydrogen-Y (H-Y) zeolite. The decomposition of submonolayer coverages of formic acid on these zeolites yields almost exclusively CO and H_2O . Both zeolites have the faujasite-type structure containing nearly spherical cavities 12 \AA in diameter interconnected by 8 to 9 \AA openings (3). The ultrastable H-Y is the "deep-bed" calcination product of the $\text{NH}_4\text{-Y}$ zeolite at about 775 K (4). Although derived from the $\text{NH}_4\text{-Y}$ zeolite, the ultrastable H-Y zeolite is quite different, possessing increased catalytic properties, increased thermal stability, and increased resistance to acid decomposition (5). It is proposed that the increased stability is the result of the removal of a portion of the tetrahedrally coordinated framework aluminum atoms, yielding cationic aluminum species with charges ranging from 1 to 3 (6). Specifically, it is suggested that the decomposition of the $\text{NH}_4\text{-Y}$ to the ultrastable H-Y zeolite creates 9 to 15 aluminum cations per unit cell (6). This is consistent with ammonia adsorption studies on the ultrastable H-Y zeolite which indicate the presence of 12 new Brønsted acid sites per unit cell (6). However, although it is generally accepted that chemical analysis combined with X-ray

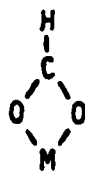
diffraction of the zeolite suggest an aluminum-deficient structure, the nature of the nonframework aluminum and the defect site is still quite uncertain (7).

The adsorbed state of formic acid on metal oxides has been studied by various spectroscopies, primarily by transmission infrared techniques (8,9,10,11). Other techniques include reflectance infrared (12), inelastic electron tunneling spectroscopy (IETS) (13,14), and nuclear magnetic resonance methods (11,15). It is the general conclusion that the formic acid chemisorbs onto metal oxides via the loss of the acidic proton. The formate ion is then bonded to the substrate through one or both of the oxygen atoms. However, there is some discussion regarding the role of the formate ion in the decomposition reaction. Some studies indicate that the rate-determining step for the reaction on alumina is the direct decomposition of the formate ion (9), whereas others maintain that the formate ions first desorb from the alumina as formic acid and then react with surface protons (10).

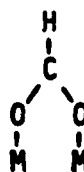
The adsorbed state of the formate ion is important in either the direct-decomposition or the desorption-and-decomposition reaction paths. The state of the formate ion may be described by any one, or a combination, of the species shown below.



I



II



III

The unidentate formate structure (species I) is bonded through a single

oxygen atom, as in formic acid and formate esters. The bidentate and bridging bidentate structures (species II and III) may occur in both symmetrical and unsymmetrical forms, depending on the metal ion lattice spacings. Infrared studies on formate salts suggest that the formate bonding is determined by the ionic radius of the metal atom (16), the electronegativity of the metal (17), or both properties plus the mass of the metal atom (18).

Because of the lack of periodicity and low concentrations of the formate ions on the polycrystalline zeolite samples, it is not feasible to determine directly the structure of the adsorbate by various diffraction methods (19). It is, therefore, necessary to examine other quantities which are sensitive to the molecular geometry and then, through analogy with known structures, determine the state of the adsorbed species. In the paper we will examine one such property, the vibrational spectra of the adsorbed formic acid, with transmission infrared spectroscopy. To aid in the assignment of the infrared bands, we will compare the spectra of the normal formic acid and the ^{13}C -enriched compound to observe the isotopic frequency shifts. In an accompanying paper, we measure another property, the chemical shift tensor, with nuclear magnetic resonance techniques (15).

II. EXPERIMENTAL PROCEDURE

The ammonium-Y (NH_4 -Y) zeolite, unit cell formula $\text{Na}_2(\text{NH}_4)_{48}(\text{AlO}_2)_{50}(\text{SiO}_2)_{142} \cdot 267\text{H}_2\text{O}$, was prepared by ion exchange with a sodium-Y zeolite. This NH_4 -Y zeolite was calcined at 775 K to yield a "deep bed" product, the ultrastable hydrogen-Y (H-Y) zeolite, with unit cell formula $\text{Na}_2\text{H}_{48}(\text{AlO}_2)_{50}(\text{SiO}_2)_{142} \cdot 26\text{H}_2\text{O}$ (4).

The zeolites were outgassed and dosed with formic acid in a sample cell described previously (3), which was designed for transmission infrared spectroscopy through powdered substrates. It was not feasible to spray a water/acetone suspension of the zeolite onto the hot CaF_2 -windowed flange, as has been done for alumina samples (20,21). Rather, a thin layer was deposited onto the CaF_2 window by sifting the zeolite through a 100-mesh sieve (0.147 mm openings). The surface density of the sifted zeolite powders was typically 4 to 5 mg/cm^2 . Taking care not to disturb the zeolite film, the cell is assembled, evacuated, and heated, with the CaF_2 flange supported horizontally. After cooling, the zeolite layer adheres to the CaF_2 window and the cell may be rotated to a vertical position to be placed in the infrared beam without loss of material. However, such deposits are not so rugged as the sprayed crusts and still require gentle handling.

The zeolites were outgassed on an ion-pumped all-metal vacuum system described previously (21). The samples were warmed at a rate of about 1 K/min while being pumped continuously. The NH_4 -Y zeolite was outgassed at 395 K for 3 hours, sufficiently cool to ensure that the ammonium ions do not decompose (22). The ultrastable H-Y zeolite was first re-calcined in a furnace at 775 K for 6 hours, cooled to about 450 K, and then sifted onto the CaF_2 flange while still warm. The cell was then assembled and the ultrastable H-Y zeolite was outgassed at 500 K for 3 hours. The typical background pressure of the cooled, outgassed substrate was 10^{-6} Torr (1 Torr = 133.3 Nm^{-2}).

The BET surface area measurements and the formic acid adsorptions

were carried out on a liquid nitrogen-trapped diffusion-pumped glass vacuum system. The nitrogen BET surface areas of the zeolites are $459 \pm 10 \text{ m}^2/\text{g}$ and $515 \pm 10 \text{ m}^2/\text{g}$ for the $\text{NH}_4\text{-Y}$ and the ultrastable H-Y, respectively, representing monolayers of about 63 and 84 nitrogen molecules per unit cell. The formic acid adsorption isotherms for both zeolites, shown in Figure 1, reveal monolayer coverages of 75 and 56 formic acid molecules per unit cell, or 5.7×10^{14} and 5.5×10^{14} molecules/ cm^2 , for the $\text{NH}_4\text{-Y}$ and the ultrastable H-Y zeolites, respectively. The formic acid was adsorbed from the gas phase. The predetermined pressure of the vapor to be adsorbed was calculated from the monomer/dimer equilibrium data of Coolidge (23). The continuous uptake of formic acid by the $\text{NH}_4\text{-Y}$ zeolite for P/P_0 greater than 0.22 suggests that the zeolite is decomposing under acid attack. The ultrastable H-Y exhibits no such degradation in the pressures studied ($P/P_0 < 0.5$). For coverages less than 40 molecules per unit cell, the equilibrium pressure of the formic acid was less than 0.1 Torr, below the range of the Wallace and Tiernan gauge used in the adsorption studies. A mass spectrometric analysis of the formic acid desorption products from a submonolayer coverage on the ultrastable H-Y at 525 K revealed that the carbon was evolved as 98.5% CO and 1.5% CO_2 with no trace on any residual formic acid detected.

The infrared spectra were measured at submonolayer coverages of formic acid adsorbed on the zeolites. In this range, though there were subtle changes in relative peak intensities, no new features developed at higher coverages. For each zeolite, we report here the spectra of two typical coverages. Specifically, the $\text{NH}_4\text{-Y}$ zeolite sample contained

about 20 molecules per unit cell. The formic acid coverage on the NH_4 -Y zeolite is well below the levels which caused structural degradation of the zeolite. The ratio of hydrogen ions formed during the adsorption to the number of ammonium ions is still low enough to allow the zeolitic framework to remain intact (24). The ultrastable H-Y sample contained about 17 formic acid molecules per unit cell.

The transmission-infrared spectra were measured with a Perkin-Elmer Model 180 spectrometer, operated in the double-beam mode. The resolution in the 1800 to 1200 cm^{-1} region was set at 2.1 cm^{-1} . The frequencies were calibrated with liquid films of the formic acid isotopes.

The ^{12}C formic acid was treated with anhydrous CuSO_4 to remove any water. The isotopically enriched formic acid (91.2% ^{13}C), obtained from Merck Isotopes, was used without further purification.

III. RESULTS

For comparison, the spectral features of the two formic acid isotopes are listed in Table 1. The samples were prepared by filling an empty infrared cell to the saturation pressure of formic acid, thus forming a liquid film on the CaF_2 windows. The band assignments in Table 1 were determined previously through an analysis of the isotopic shifts of the various deuterated forms of formic acid relative to the normal compound (25). The asymmetric vibration of the molecule (C=O stretch) exhibits the most pronounced effect upon the substitution of ^{13}C , decreasing by about 41 cm^{-1} . The symmetric vibration (C-O stretch) is somewhat less perturbed, decreasing by only 9 cm^{-1} .

The infrared spectra at 295 K of the outgassed NH_4 -Y and the ultrastable H-Y zeolites are shown in Figure 2. The surface coverages

on the CaF_2 windows were 3.8 and 4.6 mg/cm^2 for the NH_4 -Y and the ultrastable H-Y zeolites, respectively, for the two spectra shown. The spectral features of the NH_4 -Y zeolite at 1470 and 1430 cm^{-1} have been identified previously as ν_4 bending vibrations of NH_4^+ ions (22). The peak at 1670 cm^{-1} peak on the NH_4 -Y zeolite has been assigned to the bending vibration of H_2O , and the peak at 1705 cm^{-1} on the ultrastable H-Y has been associated with H_3O^+ ions (22). The infrared spectral region for both zeolites was about 2000 cm^{-1} to 1000 cm^{-1} . Above this range, 4000 cm^{-1} to 2000 cm^{-1} , there were prohibitively large losses in transmittance due to scattering. Below 1000 cm^{-1} , the spectrum was blacked out by the strong absorbances of the zeolite substrate.

The infrared spectra for formic acid adsorbed on the NH_4 -Y and ultrastable H-Y zeolites are shown in Figures 3 and 4, respectively. The spectra were obtained by subtracting the appropriate background spectra in Figure 2 from the observed spectra. In both Figures 3 and 4, spectrum (a) is the normal formic acid, and spectrum (b) is the 91% ^{13}C -enriched compound. The wavenumber markers are included only as references and are not to be taken literally as the exact assignments of the broad peaks and sidebands. Although each spectrum is composed of a number of overlapping bands, it is possible to identify the peaks due to carbon-oxygen stretches or carbon-hydrogen bands by comparison with the isotopically shifted spectrum. The shifts indicated in Figures 3 and 4 were determined by assuming that if

the intensity at a specific frequency decreased upon the substitution of ^{13}C for ^{12}C , the intensity shifted to a lower frequency, but not more than about 40 cm^{-1} for peaks in the range 1800 to 1500 cm^{-1} , and not more than about 10 cm^{-1} for peaks in the range 1500 to 1200 cm^{-1} . This analysis is rather straightforward in the ultrastable H-Y spectra, but it is slightly more arbitrary for the $\text{NH}_4\text{-Y}$ case. For example, in Figure 3, the structure at 1734 cm^{-1} of spectrum 3(a) has shifted in spectrum 3(b). Using the above guidelines, we propose that the peak has shifted to about 1698 cm^{-1} , a 34 cm^{-1} decrease, and has not shifted to about 1642 cm^{-1} , a decrease of 92 cm^{-1} .

IV. DISCUSSION

Upon isotopic substitution of ^{13}C -enriched formic acid, almost all of the peaks in the spectra of Figures 3 and 4 shift to lower frequencies. In addition, all the high frequency peaks (1750 to 1500 cm^{-1}) have corresponding peaks within 40 cm^{-1} and all the lower frequency peaks (1450 to 1200 cm^{-1}) have corresponding peaks within about 10 cm^{-1} . This is consistent with the observed isotopic shifts of formic acid. Thus, almost all of the features observed in the range 1800 to 1200 cm^{-1} of the infrared spectra of the adsorbed formic acid can be attributed to either carbon-oxygen stretches or carbon-hydrogen bending modes. The other unshifting

peaks can also be assigned to surface formate structures on the basis of their location, as will be discussed later. To interpret the positions of the infrared bands, the spectra of the formate ion in various configurations, as well as adsorbed on surfaces, will be discussed.

The relative positions of the symmetric and asymmetric stretches in the formate structure are indicative of the molecular geometry. For the covalently bonded unidentate structures of formic acid and methyl formate, the two bands are separated by 635 and 560 cm^{-1} , respectively. Upon transformation to the bidentate structure of formate salts, the carbon-oxygen double bond is weakened and the carbon-oxygen single bond is strengthened. Consequently, the separation between the two bands for typical formate salts is decreased to about 230 cm^{-1} . The infrared absorbances for some representative formate structures are given in Table 2.

The correlation between the shifts in the infrared bands and the structure of the formate group has been invoked in previous vibrational studies to differentiate between chemically and physically adsorbed formic acid. Table 3 contains the vibrational spectra of formic acid adsorbed on Al_2O_3 and other surfaces. This is by no means a comprehensive review, but rather a representative survey of previous studies to demonstrate the trends of the observed frequencies. In general, the surface formate ion has an asymmetric stretch in the range 1590 to 1625 cm^{-1} and a symmetric stretch in the range 1360 to 1468 cm^{-1} . These frequencies are in good agreement with those of the formate salts, such as the compounds listed in Table 2. On the basis of the similarities with the infrared spectra of

formate ions in metal salts, it has been proposed that the formate ion is adsorbed on the surface as symmetric bidentate structures (19).

When there is only a slight perturbation in the asymmetric band, it is usually proposed that the formic acid is physically adsorbed on the surface (8,11,14). This is most likely the case for formic acid adsorbed on Al_2O_3 at 77 K, which converts to the chemisorbed formate ion upon warming to room temperature (14). However, we propose that in the case of formic acid adsorbed on SiO_2 (11) and the Na-Y zeolite (8) at room temperature, another interpretation of the small shift in the asymmetric frequency is possible. That is, the acid may be dissociatively adsorbed on the surface in a covalently bonded unidentate structure. This is supported by a proton nuclear magnetic resonance study of the formic acid adsorbed on SiO_2 which detected only the carbonyl proton (11). It is probable that the acidic proton had dissociated from the acid and had bonded to the SiO_2 surface. Thus, if the proton were still bonded to the acid it would probably appear in the NMR spectrum, whereas if the proton had bonded to the surface, the spectrum would be extremely broadened and thus not be observed. The formate group could be bonded to the surface through a single oxygen atom to a Si or Al atom of the substrate. In this configuration, one would expect that the asymmetric band of the formic acid at 1743 cm^{-1} would be decreased only slightly, as in the case of methyl formate. Thus, we maintain that there is equal evidence for the unidentate structure as well as physically adsorbed formic acid. However, when the vibrational spectra show no evidence of formic acid OH stretches at about 3580 cm^{-1} or OH bends at about 1218 cm^{-1} , the unidentate structure is strongly implied.

The infrared spectra of formic acid adsorbed on the $\text{NH}_4\text{-Y}$ and the ultrastable H-Y zeolites have peaks extending from the physically adsorbed (or unidentate) region (about 1720 cm^{-1}) to the chemisorbed formate ion region (about 1590 cm^{-1}). The spectrum of the formic acid adsorbed on the ultrastable H-Y zeolite affords the more straightforward analysis. The most intense peaks at 1610 and 1385 cm^{-1} are assigned to the asymmetric and symmetric stretches of the formate ion, consistent with the assignments in Table 3. These bands are in close agreement with those of aluminum formate, listed in Table 2. Since there was no evidence of OH bending modes of the formic acid molecule and the adsorption isotherm suggests that the formic acid chemisorbs to the surface, the peaks at 1760 and 1718 cm^{-1} are interpreted to be the asymmetric and symmetric stretches of two unidentate formate structures. The corresponding symmetric stretches of these species are probably combined in the side peak at 1336 cm^{-1} , although it is at a higher frequency than would be expected. The 1416 cm^{-1} side peak is interpreted as the CH bend of all the adsorbed formate species.

The spectrum of the formic acid adsorbed on the $\text{NH}_4\text{-Y}$ zeolite is more complex and does not immediately suggest an obvious assignment of the various peaks. However, it is possible to compare the general shape of the spectrum to that of the ultrastable H-Y sample. In the region of the asymmetric stretch the maximum intensity has shifted from 1610 cm^{-1} to higher frequencies, near 1694 and 1734 cm^{-1} . Simultaneously, the maximum intensity in the symmetric stretch region has shifted to a lower frequency, from 1385 to 1292 cm^{-1} . Thus, assuming that the extinction coefficients

of each peak do not change radically from the ultrastable H-Y to the NH_4 -Y zeolite, the infrared spectra suggest that the NH_4 -Y sample contains a larger percentage of unidentate formate groups.

The new peaks that appear in the spectrum of the formic acid adsorbed on the NH_4 -Y sample are tentatively interpreted as follows. The minimum at 1762 cm^{-1} may be only the initial slope of a large dip in the background spectrum caused by the loss of NH_4^+ ions upon the adsorption of formic acid. The 1534 and 1454 cm^{-1} peaks involve the carbon atom since they are shifted upon isotopic substitution. These bands do not have analogies in any of the formate compounds although it is possible that the band at 1454 cm^{-1} is related to the 1468 cm^{-1} band observed for formic acid on Al_2O_3 (13,14).

V. CONCLUSIONS

Vibrational spectra observed by transmission infrared spectroscopy and adsorption isotherms suggest that formic acid chemically adsorbs on the surface of the NH_4 -Y and ultrastable H-Y zeolites in at least two configurations. These two structures have been interpreted to be a covalently bonded unidentate formate group and as a formate ion. Based on the position of the bands assigned to the formate ion and the agreement with the bands of aluminum formate, it is likely that the formate ion has a bidentate structure. It was not possible to determine if the formate ion is adsorbed as a bidentate or bridging-bidentate species. The presence of the unidentate formate group, as opposed to physically adsorbed formic acid, is supported by the adsorption isotherms and the lack of any OH bending vibrations in the infrared spectra. The unidentate structure is probably covalently bonded, similar to ester compounds, to

account for the position of the infrared bands near 1734 and 1694 cm^{-1} . The frequencies of the asymmetric stretches of unidentate salts are generally not this high (27), whereas unidentate-type esters such as methyl formate are all within this range. Although there is no direct experimental evidence to suggest it, the unidentate species would be more likely to form at the Si atoms of the zeolite since the aluminum formate is known to have a bidentate structure (27).

The adsorption of formic acid is markedly different on the NH_4 -Y and ultrastable H-Y zeolites. As revealed by the infrared spectra, the formic acid is adsorbed on the ultrastable H-Y zeolite primarily as formate ions, whereas on the NH_4 -Y zeolite, the unidentate species appears to be slightly in the majority. Both zeolites have the faujasite structure and there is no infrared evidence of surface hydroxyl groups on either zeolite. However, the ultrastable H-Y zeolite is suggested to contain a number of non-framework aluminum ions in the supercages (6). Therefore it is likely that the increased proportion of formate ions on the ultrastable H-Y zeolite is due to the presence of the aluminum ions which act as adsorption sites for the formic acid. Further studies are required to determine if these sites are responsible for the enhanced catalytic properties of the ultrastable H-Y zeolite.

These conclusions will be further examined in an accompanying paper (15), in which nuclear magnetic resonance techniques are applied to study the state of the adsorbed formic acid molecule, the nature of the adsorption site, and the relative populations of these sites.

VI. ACKNOWLEDGMENTS

The authors gratefully acknowledge support from the Office of Naval Research under contract N00014-75-C-0960. We thank Professor George R. Rossman for his kindness in allowing us to use his infrared spectrometer and Dr. G. T. Kerr of Mobil Oil Research and Development for supplying the zeolite samples. Professor W. H. Weinberg and Professor S. I. Chan offered helpful discussions and suggestions on the manuscript.

References

1. P. Mars, J. J. F. Scholten, and P. Zweitering, *Adv. Catal.* 14, 35 (1963).
2. J. M. Trillo, G. Munuera, and J. M. Cridao, *Catal. Rev.* 7, 51 (1973).
3. P. B. Venuto and P. S. Landis, *Adv. Catal.* 18, 259 (1968).
4. (a) G. T. Kerr, *Adv. in Chem. Series* 121, 219 (1973);
(b) C. V. McDaniel and P. K. Maher, Molecular Sieves, Soc. of the Chem. Industry, London, 1967, p. 86.
5. M. L. Poutsma, Zeolite Chemistry and Catalysis, J. A. Rabo, ed., ACS Monograph 171, 1976, p. 437.
6. G. T. Kerr, *J. Catalysis* 15, 200 (1969).
7. J. V. Smith, Zeolite Chemistry and Catalysis, J. A. Rabo, ed., ACS Monograph 171, 1976, p. 56.
8. A. Bielanski and J. Datka, *J. Catalysis* 32, 183 (1974).
9. J. J. F. Scholten, P. Mars, P. G. Menon, and R. Van Hardeveld, *Proc. Intern. Cong. Catalysis*, 3rd, Amsterdam, 1964, p. 881.
10. Y. Noto, K. Fukuda, T. Onishi, and K. Tamaru, *Trans. Far. Soc.* 63, 2300 (1967).
11. K. Hirota, K. Fueki, K. Shindo, and Y. Nakai, *Bull. Chem. Soc. Japan* 32, 1261 (1959).
12. M. Ito and W. Suetaka, *J. Phys. Chem.* 79, 1190 (1975).
13. B. F. Lewis, M. Mosesman, and W. H. Weinberg, *Surface Sci.* 41, 142 (1974).
14. O. I. Shklyarevskii, A. A. Lysykh, and I. K. Yanson, *Sov. J. Low. Temp. Phys.* 2, 328 (1976).

15. T. M. Duncan and R. W. Vaughan, *J. Catalysis*, submitted.
16. R. Theimer and O. Theimer, *Monatsh.* 81, 313 (1950).
17. B. Ellis and H. Pyszora, *Nature* 181, 181 (1958).
18. R. E. Kagarise, *J. Phys. Chem.* 59, 271 (1955).
19. J. T. Hall and P. K. Hansma, *Surface Sci.* 76, 61 (1978).
20. R. G. Greenler, *J. Chem. Phys.* 37, 2094 (1962).
21. J. T. Yates, Jr., T. M. Duncan, S. D. Worley, and R. W. Vaughan, *J. Chem. Phys.* 70, 1219 (1979).
22. J. B. Uytterhoeven, L. G. Christner, and W. K. Hall, *J. Phys. Chem.* 69, 2117 (1965).
23. A. S. Coolidge, *J. Amer. Chem. Soc.* 50, 2166 (1928).
24. C. V. McDaniel and P. K. Maher, *Zeolite Chemistry and Catalysis*, J. A. Rabo, ed., ACS Monograph 171, 1976, p. 296.
25. R. C. Millikan and K. S. Pitzer, *J. Chem. Phys.* 27, 1305 (1957).
26. A. R. Katritzky, J. M. Lagowski, and J. A. T. Beard, *Spectrochim. Acta* 16, 964 (1960).
27. J. D. Donaldson, J. F. Knifton, J. O'Donoghue, and S. D. Ross, *Spectrochim. Acta* 20, 847 (1964).

TABLE 1

Vibrational Spectra^(a) of H¹²COOH and H¹³COOH^(b)

| <u>Assignment</u> ^(c) | <u>H¹²COOH</u> | <u>H¹³COOH</u> | <u>$\Delta\nu$</u> |
|----------------------------------|---------------------------|---------------------------|-------------------------------|
| O-H stretch | 3580 | 3580 | 0 |
| C-H stretch | { 2943 2938 } | { 2934 2927 } | { -9 -11 } |
| C=O stretch | { 1746 1736 } | { 1705 1694 } | { -41 -42 } |
| C-O stretch | 1106 | 1097 | -9 |
| C-H bend | 1362 | 1351 | -11 |
| O-H bend | 1218 | 1206 | -12 |

(a) all frequencies in wavenumbers, cm^{-1}

(b) monomer form of the acid in a liquid film.

(c) based on band assignments in Reference 25.

TABLE 2

Vibrational Spectra of Formate Compounds^(a)

| <u>Compound</u> | <u>$\nu(\text{C=O})$</u> | <u>$\nu(\text{C-O})$</u> | <u>$\delta(\text{CH})$</u> | <u>Reference</u> |
|-------------------------------------|-------------------------------------|-------------------------------------|---------------------------------------|------------------|
| HCOOH | 1741 | 1106 | 1362 | This work |
| HCOOCH ₃ ^(b) | 1722 | 1162 | 1377 | 26 |
| Na(HCO ₂) | 1592 | 1364 | 1381 | 27 |
| NH ₄ (HCO ₂) | 1592 | 1364 | 1406 | 27 |
| Al(HCO ₂) ₃ | 1613 | { 1387 1368 } | { 1420 1406 } | 27 |

(a) all frequencies in wavenumbers, cm^{-1}

(b) HCOOCH₃ in CHCl₃ solution

TABLE 3

Representative Vibrational Band Positions for Adsorbed Formic AcidA. Chemically Adsorbed Formate Ions

| <u>Substrate</u> | <u>Vibrational Band Assignments (a)</u> | | | <u>Measurement Technique</u> | <u>Reference</u> |
|--------------------------------|---|--------------------|----------------|------------------------------|------------------|
| | <u>C=O Stretch</u> | <u>C-O Stretch</u> | <u>CH Bend</u> | | |
| Al Metal | 1590 | 1360 | - | Reflectance Infrared | 12 |
| Al ₂ O ₃ | 1597 | 1377 | - | Transmission Infrared | 20 |
| Al ₂ O ₃ | 1600 | 1380 | - | Transmission Infrared | 9 |
| Al ₂ O ₃ | 1625 | 1390 | 1407 | Transmission Infrared | 10 |
| Al ₂ O ₃ | 1620 | 1344 | 1402 | Transmission Infrared | 11 |
| Na-Y Zeolite | - | 1385 | - | Transmission Infrared | 8 |
| Al ₂ O ₃ | 1621 | 1468 | 1390 | IETS | 13 |
| Al ₂ O ₃ | 1620 | 1468 | 1390 | IETS | 14 |
| | | 1320 | | | |

B. Physically Adsorbed Formic Acid

| | | | | | |
|--|------|------|------|-----------------------|----|
| Al ₂ O ₃ at 77 K | 1700 | 1250 | 1390 | IETS | 14 |
| S10 ₂ | 1714 | 960 | - | Transmission Infrared | 11 |
| Na-Y Zeolite | 1720 | - | - | Transmission Infrared | 8 |

(a) all frequencies in cm⁻¹

Figure Captions

- Figure 1. Adsorption isotherms for formic acid on the $\text{NH}_4\text{-Y}$ (\square) and the ultrastable H-Y (Δ) zeolites at 297 K.
- Figure 2. Background infrared spectra for the $\text{NH}_4\text{-Y}$ and ultrastable H-Y zeolites.
- Figure 3. Background-corrected infrared spectra of formic acid ((a) H^{12}COOH and (b) H^{13}COOH) adsorbed on the $\text{NH}_4\text{-Y}$ zeolite at 295 K.
- Figure 4. Background-corrected infrared spectra of formic acid ((a) H^{12}COOH and (b) H^{13}COOH) adsorbed on the ultrastable H-Y zeolite.

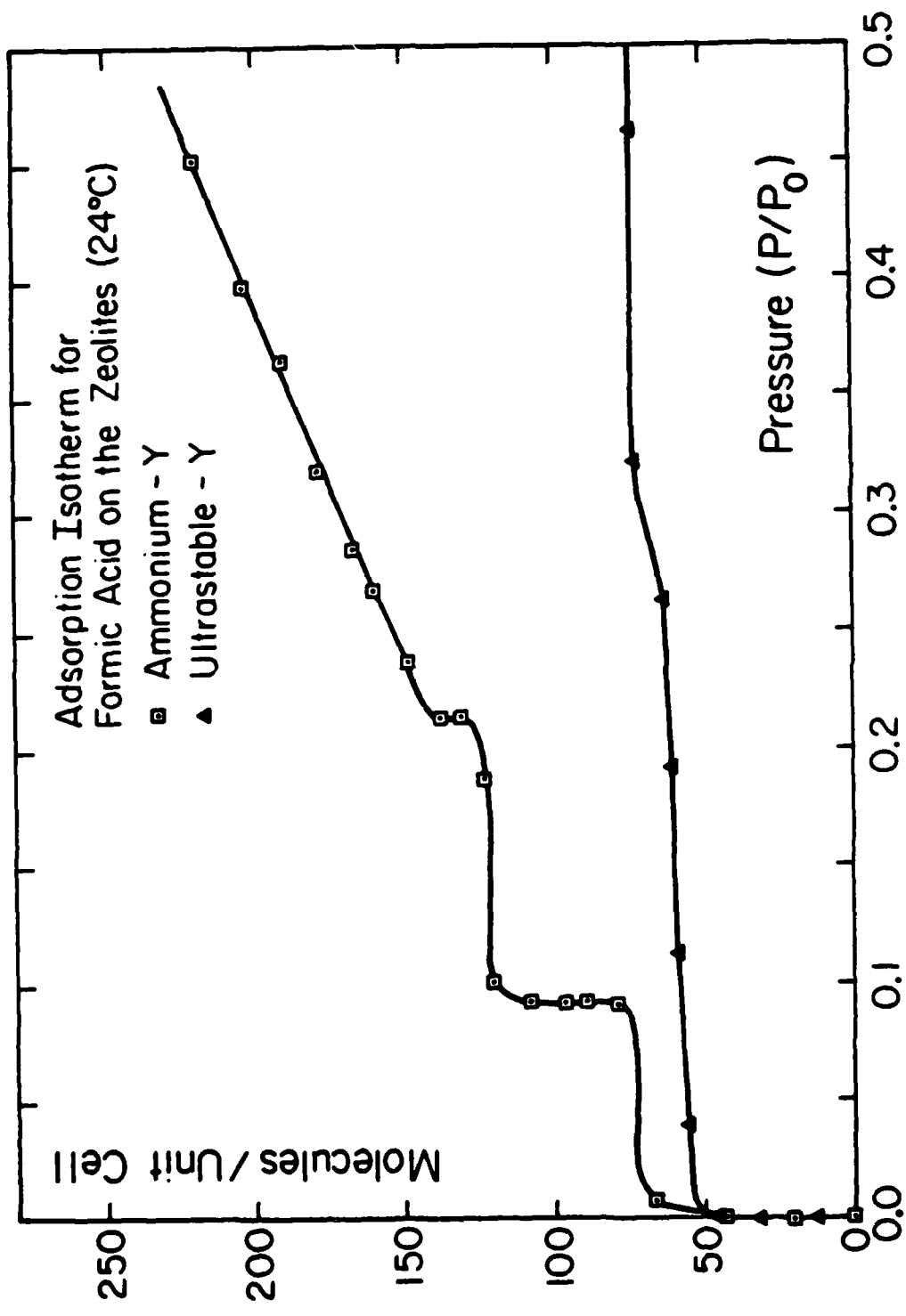


Figure 1.

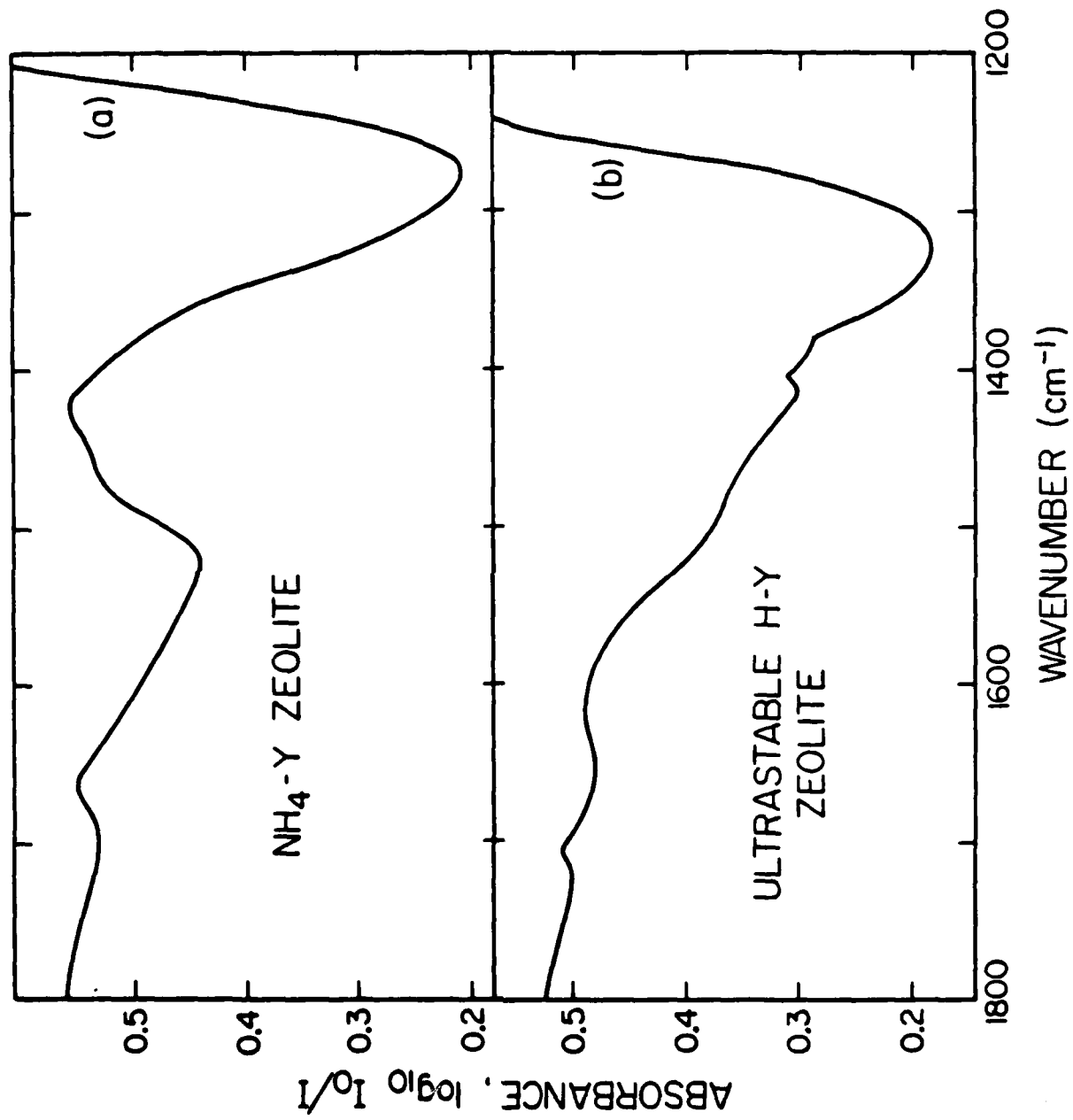


Figure 2.

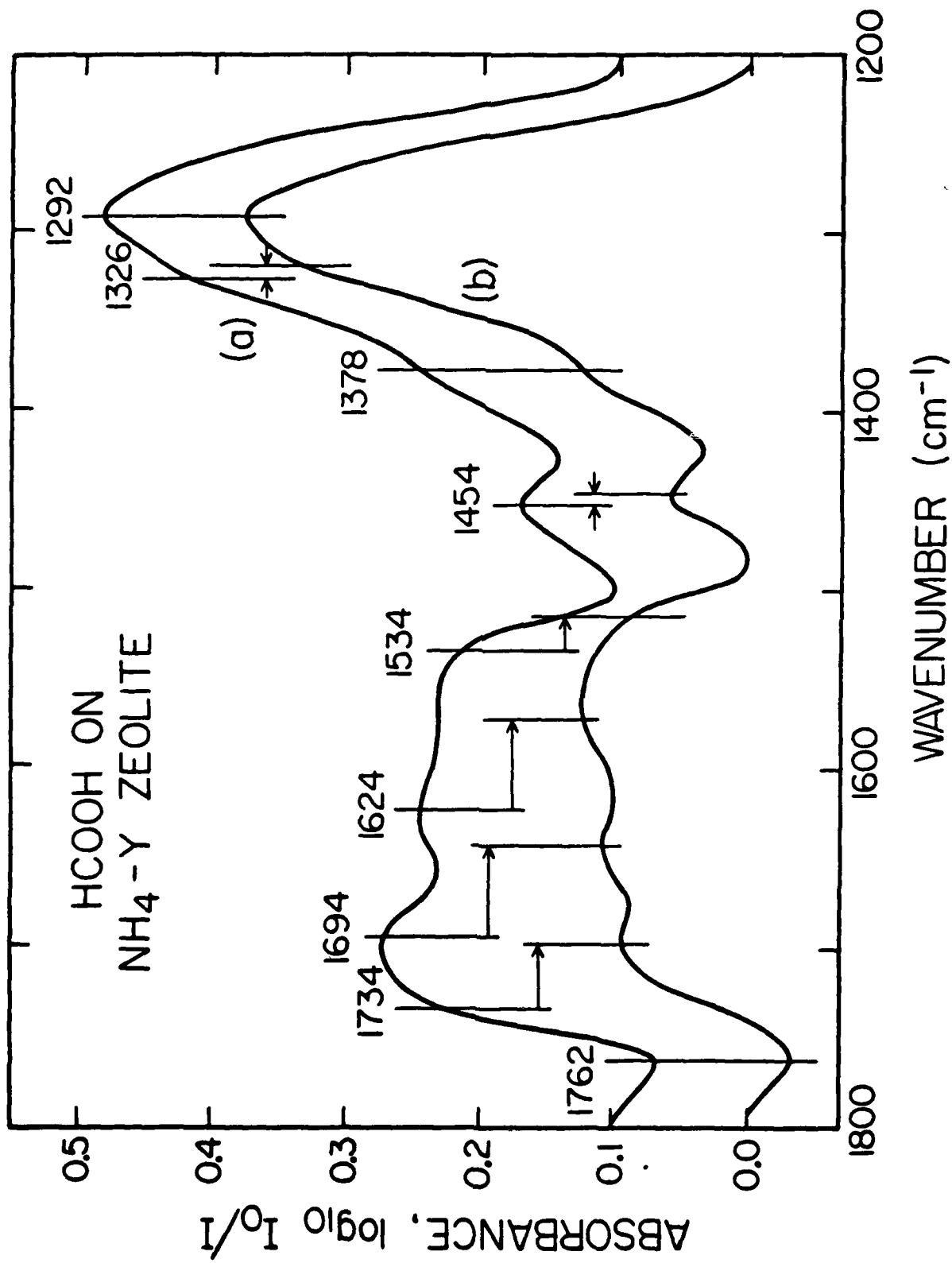


Figure 3.

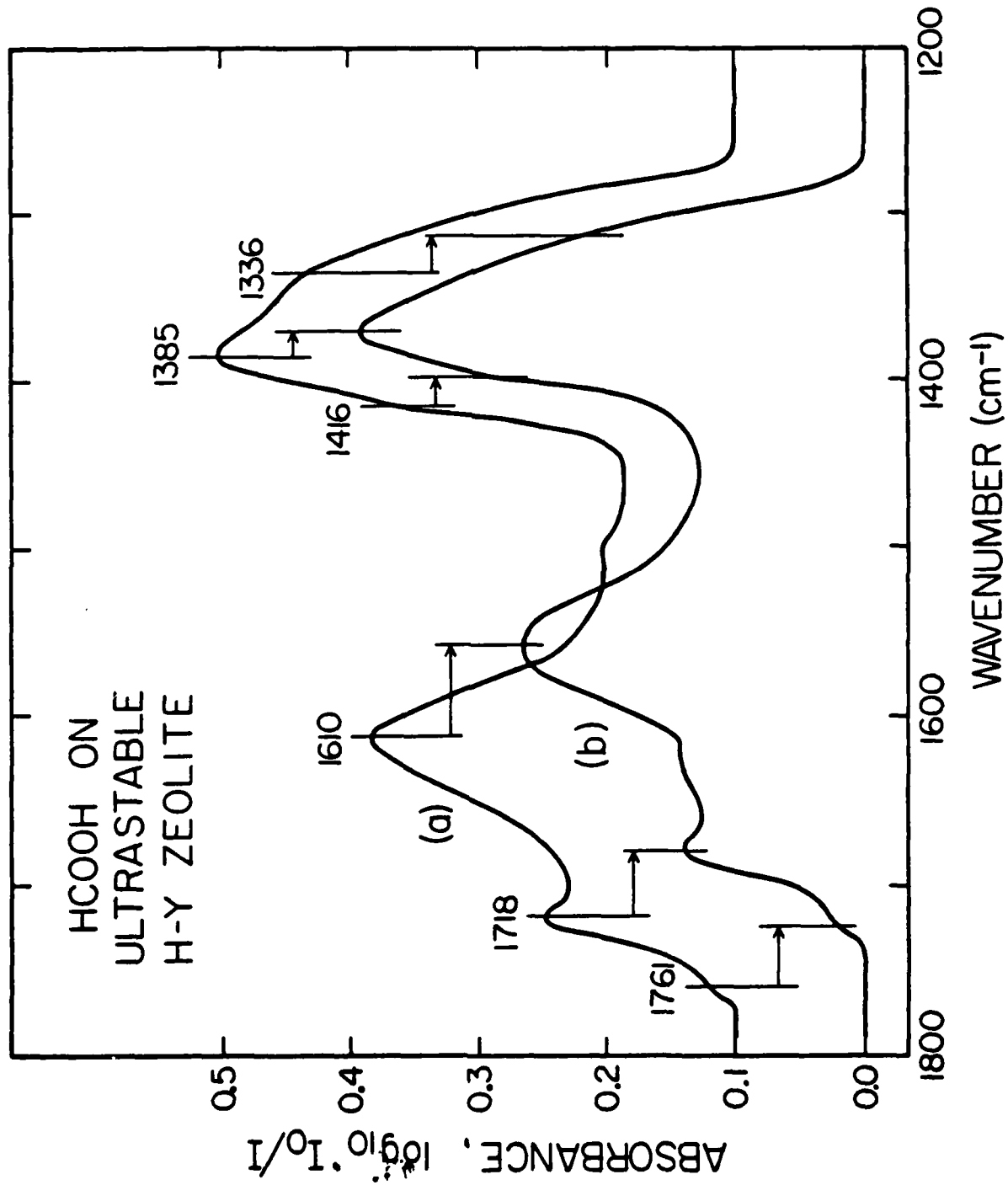


Figure 4.